

Bacteriophage genes that inactivate the CRISPR/Cas bacterial immune system

Joe Bondy-Denomy¹, April Pawluk², Karen L. Maxwell³, and Alan R. Davidson^{1,2,*}

¹Department of Molecular Genetics, University of Toronto, Toronto, Ontario, Canada M5S 1A8

²Department of Biochemistry, University of Toronto, Toronto, Ontario, Canada M5S 1A8

³Donnelly Centre for Cellular and Biomolecular Research, University of Toronto, Toronto, Ontario, Canada M5S 3E1

A widespread system used by bacteria for protection against potentially dangerous foreign DNA molecules are the clustered regularly interspaced short palindromic repeats (CRISPR) loci coupled with *cas* (CRISPR-associated) genes¹. Similar to RNA interference (RNAi) in eukaryotes², these CRISPR/Cas systems utilize small RNAs for sequence-specific detection and neutralization of invading genomes³. Here we describe the first examples of genes that mediate the inhibition of a CRISPR/Cas system. Five distinct “anti-CRISPR” genes were found in the genomes of phages infecting *Pseudomonas aeruginosa*. Mutation of the anti-CRISPR gene of a phage rendered it unable to infect bacteria with a functional CRISPR/Cas system, and the addition of the same gene to the genome of a CRISPR/Cas-targeted phage allowed it to evade the CRISPR/Cas system. Phage-encoded anti-CRISPR genes may represent a widespread mechanism for phages to overcome the highly prevalent CRISPR/Cas systems. The existence of anti-CRISPR genes presents new avenues for the elucidation of CRISPR/Cas functional mechanisms and provides new insight into the co-evolution of phages and bacteria.

Predation by phages presents a major challenge to bacterial survival⁴, and bacteria have evolved numerous mechanisms to resist phage infection⁵. One such system is the CRISPR/Cas immune system, which is found in 48% of eubacteria and 95% of archaea⁶. CRISPR loci contain multiple repeated sequences of approximately 30 base pairs, separated by variable “spacer” sequences of similar length, which are often identical to segments of phage genomes or other mobile genetic elements⁶. The large single transcript from a CRISPR locus is processed within the repeat regions into small CRISPR RNAs (crRNAs)^{7,8} that are complexed with Cas proteins^{3,9}. Using the crRNAs as guides, crRNA/Cas complexes cleave foreign DNA molecules at sites bearing complementarity to the crRNAs,

Reprints and permissions information is available at www.nature.com/reprints.

*Correspondence and requests for materials should be addressed to A.R.D. (alan.davidson@utoronto.ca).

Author Contributions

J.B.D. designed experiments, performed experiments and wrote the manuscript, A.P. performed experiments, K.L.M. supervised experiments, and A.R.D. designed experiments and wrote the manuscript.

Newly sequenced phage genomes are deposited at NCBI under the following accession numbers: JX434030 (JBD5), JX434031 (JBD24), JX434032 (JBD30), and JX434033 (JBD88a).

thus engendering resistance to phages and other invading DNA molecules^{10,11}. Cas proteins also mediate an adaptive function by incorporating short sequences (i.e. a new spacer) from newly encountered foreign genomes into CRISPR loci so that these genomes will be destroyed in subsequent encounters^{12–14}. The relatively recent elucidation of CRISPR/Cas functions and their obvious similarities to RNAi systems of eukaryotes have led to vigorous investigation of these systems.

Since phage genes have been discovered that can neutralize most of the prevalent bacterial anti-phage defences⁵, the failure to identify genes that counteract the widely occurring CRISPR/Cas systems was surprising. To search for such “anti-CRISPR” activity, we investigated the Type I-F CRISPR/Cas system¹ of the opportunistic pathogen *Pseudomonas aeruginosa*¹⁴ utilizing a collection of 44 lysogens of *P. aeruginosa* PA14, which each contained a different phage genome (see Methods). In lysogens, phage genomes are integrated into the bacterial genome and are referred to as prophages. Although prophage genes are generally repressed, all prophages have some genes that are actively transcribed. To test whether prophages might express anti-CRISPR activity, we measured the plaquing efficiency of three “CRISPR-sensitive” phages (JBD18, JBD25, and JBD67) on our collection of lysogens. The CRISPR-sensitive phages fail to replicate on PA14 due to the action of the CRISPR/Cas system¹⁴, but are able to replicate on PA14 CR/cas, which contains no CRISPR loci or cas genes (Fig. 1a, Supplementary Fig. 1a). We identified three lysogenic strains, PA14(JBD24), PA14(MP29), and PA14(JBD30), on which the CRISPR-sensitive phages could form plaques very robustly as compared to unlysogenized PA14 (Fig. 1a; Supplementary Fig. 1a). Notably, the plaquing efficiency of the CRISPR-sensitive phages on PA14(JBD30) was equivalent to that on the CR/cas strain, indicating that the JBD30 prophage caused complete inactivation of the CRISPR/Cas system. The somewhat lower plaquing efficiency of the CRISPR-sensitive phages on the other lysogens relative to their plaquing on the CR/cas strain may be due to their production of less potent anti-CRISPR activity. However, these prophages also attenuate plaquing through mechanisms independent of the CRISPR/Cas system as is demonstrated by the partial inhibition of plaquing of the control phage, DMS3, which is not affected by the CRISPR/Cas system (Fig. 1a and Supplementary Fig. 1a).

To directly assess the anti-CRISPR activity of the PA14 lysogens, we used a plasmid-based transformation efficiency assay. The sequences within phages that are targeted by the CRISPR/Cas system are called protospacers. In order to be targeted, a protospacer sequence must be complementary to a specific spacer sequence within the CRISPR locus and also possess a correct Protospacer Adjacent Motif (PAM)^{15,16} (Fig. 1b). Protospacer sequences are named according to the spacer sequence that they match in the PA14 genome (Fig. 1b). We constructed plasmids containing targeted protospacer sequences from phages JBD18 (CRISPR2 locus, spacer 1 or CR2_sp1) and JBD25 (CR1_sp1)¹⁴. The transformation efficiencies of the plasmids bearing protospacers into unlysogenized PA14 were reduced by at least 90% compared to an empty vector control, whereas no difference in transformation efficiency was seen for the three strains containing prophages expressing anti-CRISPR activity, or for the CR/cas strain (Fig. 1c). These data confirm that the prophages isolated in our screen inhibit the PA14 CRISPR/Cas system.

Genome comparisons revealed that the phages producing anti-CRISPR activity were closely related to each other, and also displayed high sequence similarity and synteny with the previously characterized *P. aeruginosa* Mu-like phages D3112, DMS3, and MP22 (Supplementary Table 1). An unusual feature of each of these genomes compared to more distantly related Mu-like phages infecting *P. aeruginosa*¹⁷ and other hosts¹⁸ is the presence of diverse atypical genes at a single position within the region encoding phage head proteins (Fig. 1d, Supplementary Fig. 2). We suspected that some of these genes might encode anti-CRISPR activities; thus, seventeen of them were cloned and expressed from a high copy number plasmid in PA14 under the control of an arabinose-inducible promoter. Remarkably, expression of seven of these genes (Supplementary Fig. 7) led to dramatic increases in the plaquing efficiency of the CRISPR-sensitive phages (Fig. 1e; Supplementary Fig. 1b). Each anti-CRISPR gene allowed these three different phages to evade the CRISPR/Cas system even though they bear distinct protospacer targets (Supplementary Table 1), indicating that the anti-CRISPR genes do not function through protection of specific DNA sequences on the phages. We also found that the anti-CRISPR genes can inhibit the Type I-F systems found in other *P. aeruginosa* strains, demonstrating that this phenomenon is not particular to strain PA14 (Supplementary Fig. 4). Finally, we found that the anti-CRISPR genes did not inhibit a Type I-E CRISPR/Cas system functioning in *E. coli*¹⁹ (Supplementary Fig. 5). Since Type I-E is the most closely related CRISPR/Cas system to Type I-F¹, we do not expect that these genes would inhibit the function of any of the other more distantly related CRISPR/Cas systems.

For the Type I-F CRISPR/Cas system to function, transcription of pre-crRNA from the CRISPR locus must occur, followed by processing into small crRNAs and incorporation of these RNAs into a complex with Cas proteins^{3,7}. The stable maintenance of processed crRNA within the cell requires Cas proteins. Thus, the lack of any *P. aeruginosa* Cas protein except Cas1, which is involved in spacer acquisition, causes a marked reduction in crRNA levels²⁰. As can be seen in Supplementary Fig. 6a, expression of five different anti-CRISPR genes within PA14 caused no change in the level of processed crRNA molecules as detected by northern blotting. The normal level of crRNA observed implies that expression of anti-CRISPR genes does not cause a reduction in the expression levels of the CRISPR loci or *cas* genes. Supporting this finding, we also showed that transcription levels of the *cas* genes *cas3* and *csy3* were unaffected by the anti-CRISPR genes as assessed by reverse transcriptase quantitative PCR (RT-qPCR) (Supplementary Fig. 6b,c). Furthermore, β -galactosidase activity produced from a chromosomally located *csy3::lacZ* fusion gene was not perturbed by expression of any of the anti-CRISPR genes (Supplementary Fig. 6d). We conclude from these experiments that the anti-CRISPR genes exert their effects at a step occurring after formation of the crRNA-Cas complex, and that there is no effect on biogenesis of either the crRNA or Cas proteins.

Despite the common genomic positions of the anti-CRISPR genes in very similar *P. aeruginosa* phages, these seven genes are predicted to encode five different proteins with completely distinct sequences (Supplementary Fig. 3). Sequence similarity searches with each of these proteins yielded fewer than 15 different significant hits in total, of which all but four were proteins encoded in genomes of closely related phages or prophages (Supplementary Table 2). One of the non-phage associated anti-CRISPR protein

homologues, which is 43% identical to the product of gene *33* of phage JBD88a (JBD88a gp33), is encoded within an active pathogenicity island of a highly virulent *P. aeruginosa* clinical isolate that is likely transferred by conjugation between *P. aeruginosa* strains²¹. This island contains 4 protospacers with correct PAMs and 100% identity to CRISPR spacers in various *P. aeruginosa* strains²². The three other non-phage associated anti-CRISPR homologues are also found in regions of *Pseudomonas* genomes that may be mobile elements as indicated by presence of genes in these regions encoding homologues of proteins involved in DNA transfer and/or Type IV secretion (Supplementary Fig. 7). Thus, these putative bacterial anti-CRISPR genes may increase the fitness for inter-strain transfer of these mobile elements by inactivating the CRISPR/Cas system of a recipient strain.

Since the crRNA/Cas complex is guided by RNA, anti-CRISPR activity might be mediated by a non-coding RNA molecule or a protein encoded by an anti-CRISPR gene. We addressed this issue by performing experiments on JBD30 gene *35*. A nonsense mutation at the third codon and two different frameshift mutations were introduced to the plasmid encoding gene *35*. Each of these mutations abrogated anti-CRISPR activity (Supplementary Fig. 8), implying that translation of this region was required for function. Since these experiments did not rule out a combined role for anti-CRISPR non-coding RNA and protein, two variant genes were synthesized that encoded the same amino acid sequence as gene *35*, yet had DNA sequences that differed by ~35% through variation of codon wobble positions (Supplementary Fig. 9). As shown in Supplementary Fig. 8, each of these synthetic versions of gene *35* imparted full anti-CRISPR activity. These data demonstrate that anti-CRISPR protein is required for anti-CRISPR activity and that a direct mechanistic role for a gene *35*-encoded RNA is unlikely.

The genomes of six of the seven “anti-CRISPR phages” (i.e. those phages bearing active anti-CRISPR genes, Fig. 1d) contain at least one functional protospacer (Supplementary Table 1); thus, their replication should be inhibited by the PA14 CRISPR/Cas system. However, each was able to form plaques on PA14 with 100% efficiency compared to the CR/cas strain (Supplementary Fig. 10). Using the transformation efficiency assay, we confirmed that the two protospacers found most commonly in the anti-CRISPR phages were indeed targeted by the PA14 CRISPR/Cas system (Supplementary Fig. 11). These results implied that the anti-CRISPR phages are able to replicate on PA14 because they possess anti-CRISPR genes. To address this hypothesis, a frameshift mutation was introduced into the phage JBD30 anti-CRISPR gene (gene *35*). This mutant phage was unable to replicate on wild-type PA14 but still replicated robustly on the CR/cas strain, demonstrating the requirement of the anti-CRISPR gene for replication in cells bearing an intact CRISPR/Cas system (Fig. 2a). To determine whether the introduction of an anti-CRISPR gene into a CRISPR-sensitive phage would allow that phage to evade CRISPR/Cas immunity, we utilized a CRISPR-sensitive mutant of phage DMS3, called DMS3*m*¹⁴. This phage possesses a functional protospacer and is very similar in sequence to the anti-CRISPR phages, yet it contains no functional anti-CRISPR gene (Fig. 1c). Taking advantage of the high DNA sequence identity between phages DMS3*m* and JBD30, *in vivo* homologous recombination was used to create a version of DMS3*m* bearing JBD30 gene *35* (Fig. 2b, Supplementary Fig. 12 and Methods). As shown in Fig. 2c, the introduction of this gene into DMS3*m* resulted in a 10⁶-fold increase in plaquing efficiency on PA14, clearly

demonstrating that an anti-CRISPR gene present on an infecting phage allows that phage to overcome the CRISPR/Cas system. By testing lysogens of the DMS3*m* and JBD30 mutant prophages we found that a protospacer-bearing plasmid transformed cells efficiently only those lysogens in which an intact anti-CRISPR gene was present (Fig. 2d). These assays demonstrate the necessity and sufficiency of the anti-CRISPR gene for inhibition of the CRISPR/Cas system.

The adaptive nature of the CRISPR/Cas system and the widespread occurrence of CRISPR regions in bacterial genomes suggest that this system could be the most powerful weapon possessed by bacteria to resist invasion by foreign DNA. Prior to our work, the only known mechanism for phages to evade CRISPR/Cas systems was by mutation^{12,23}, which is a low frequency event. Here we have provided the first demonstration that the *in vivo* activity of a CRISPR/Cas system is profoundly inhibited by any one of five different “anti-CRISPR” genes. The existence of anti-CRISPR genes is one possible explanation of how phages have continued to proliferate despite the ubiquity and potency of CRISPR/Cas systems. The possibility that anti-CRISPR genes are diverse and widespread among phages and other mobile genetic elements may account for the large diversity of CRISPR/Cas systems and the existence of multiple CRISPR/Cas system types within single bacterial strains. This proliferation of CRISPR/Cas systems may be driven by the concomitant proliferation and diversification of anti-CRISPR genes. This newly discovered arms race may have a profound effect on the evolution of both phage and bacterial genomes and knowledge of anti-CRISPR genes will be crucial for understanding this process. The failure to detect anti-CRISPR genes until now may be due only to a lack of systematic searches using naturally functioning *in vivo* systems. Future studies to discover more anti-CRISPR genes and elucidate the mechanisms of their inhibition of CRISPR/Cas systems will provide new inroads for illumination of CRISPR/Cas function.

Methods

Strains and Growth Conditions

All bacterial strains, phages, plasmids and primers used in this study are listed in Supplementary Table 3 (File 1). *Pseudomonas aeruginosa* UCBPP-PA14 (PA14), other *P. aeruginosa* isolates and *E. coli* DH5 α were grown on lysogeny broth (LB) agar or liquid medium at 37 °C. LB was supplemented with gentamicin (50 μ g/ml for *P. aeruginosa* and 15 μ g/ml for *E. coli*) to maintain the pHERD30T plasmid or ampicillin (100 μ g/ml) for *E. coli* and carbenicillin (300 μ g/ml) for *P. aeruginosa* with the pHERD20T plasmid.

Phage Induction and Isolation

Phages were isolated from a diverse panel of 88 clinical and environmental isolates of *P. aeruginosa* by inducing the resident prophages in these strains. The strains were grown at 37 °C to early-log phase (OD_{600nm}=0.5) and the DNA-damaging agent, mitomycin C (3 μ g/ml), was added to the culture to induce prophages. Treatment was allowed to continue until lysis was visible (~4–5 hours) and chloroform was added for 15 min. The lysate was centrifuged at 10,000 g for 10 min and the supernatant was kept and stored over 100 μ l of chloroform at 4 °C. These lysates were subjected to plaque assays on bacterial lawns of 20

indicator strains from the initial collection. Visible plaques indicated the presence of phage originating from a given lysate. All phages were subjected to three rounds of plaque purification before further characterization.

Plaque Assays

Plaque assays were conducted at 30 °C or 37 °C on LB agar (1.5%) plates along with LB top agar (0.7%), both supplemented with MgSO₄ (10 mM). 150 µL of an overnight culture was mixed with top agar and poured onto LB agar plates, on which phage suspensions were spotted. The observed circular zones of clearing (plaques) are due to phage replication and lysis of the bacterial host. Alternately, full plate assays were conducted where phage and bacteria were mixed, preadsorbed for 15 min at 37 °C before adding to top agar and pouring. In the images shown in this paper, 3 µL of phage were spotted in each example and the most concentrated spot contained $\sim 5 \times 10^6$ – 1×10^7 plaque forming units (pfu). For the preparation of highly pure phage stocks, phage were precipitated with 10% (w/v) polyethylene glycol (PEG) 8000, and subjected to two cesium chloride equilibrium centrifugation gradients. These preparations were used for DNA extraction and subsequent sequencing.

Lysogen Construction

Lysogens were constructed by spotting serial dilutions of phage lysate on strain PA14 and streaking out bacteria (i.e. putative lysogens) from the inside of a clearing resulting from a cluster of plaques. Colonies were then screened to confirm resistance to the phage used to lysogenize the strain. The putative lysogens were grown in liquid culture, and the presence of spontaneously produced phage in the supernatant that could plaque on the original wild-type strain confirmed lysogeny. All PA14 lysogens were constructed with phages isolated from this work (i.e. JBD phages), with the exception of phages MP22²⁶, MP29²⁷, D3112²⁸, and DMS3²⁵.

DNA Extraction/Phage Genome Sequencing

Phage genomic DNA was extracted for sequencing from 500 µL of a cesium chloride purified phage preparation with a titer between 10^{11} – 10^{12} pfu/ml. Phages were disrupted and proteolyzed by treatment with EDTA (20 mM), proteinase K (50 µg/ml), and SDS (0.5% w/v) at 56 °C for 1h, then the DNA was extracted with phenol/chloroform and precipitated with ethanol. Phage genomes were sequenced with either Illumina Solexa or 454 high-throughput sequencing. Accession numbers for phage genomes are provided in Supplementary Table 3.

Phage Genome Analysis

New phage genome sequences were first analyzed using BLASTn to assess general similarity to previously sequenced phages. To predict open reading frames and align multiple phages for comparison, the RAST program²⁹ was used. Comparison and analysis of specific phage proteins was done using RAST, CLUSTAL³⁰, or BLASTp/PSI-BLAST³⁵.

Plasmid Construction

A shuttle vector that replicates in *E. coli* and *P. aeruginosa*, pHERD30T³¹, was used for cloning and expression of genes in *P. aeruginosa*. This vector has an arabinose-inducible promoter and a selectable gentamicin marker. A related plasmid, pHERD20T, was used for the anti-CRISPR knock out and knock in experiments which is ampicillin/carbenicillin selectable. Inserts were amplified by PCR. Vector and insert were digested with the indicated restriction enzymes (Supplementary Table 3), ligated, and the ligation mix was used to transform *E. coli* DH5 α . All plasmid constructs were verified by sequencing using primers that annealed to sites outside of the multiple cloning site. Other mutations to JBD30 gene *35* were introduced using primers shown in Supplementary Table 3.

To produce versions of JBD30 gene *35* with divergent DNA sequences (JBD30–35varA and varB), sequences containing maximal numbers of silent mutations were designed manually and synthesized by GenScript USA (Piscataway, NJ). The synthesized genes were subcloned into pHERD30T by digestion with *NcoI* and *HindIII*.

Transformation Efficiency Assays

Oligonucleotides were synthesized to match a desired 32-base protospacer (Supplementary Table 3) along with the upstream and downstream 5 bases. Additional bases were added on the 5' and 3' ends of each oligonucleotide to produce *NcoI* and *HindIII* sticky ends after annealing. The oligonucleotides were annealed and ligated into the pHERD30T shuttle vector. For transformation assays into *P. aeruginosa*, standard electroporation protocols were used. 1 ml of an overnight culture was washed twice in 300 mM sucrose and concentrated 10-fold. Subsequently, 300–500 ng of plasmid were electroporated then the cells were incubated in antibiotic-free LB medium for 1 h at 37 °C. Cells were plated on gentamicin (50 μ g/ml) selective media and colonies were counted after overnight growth at 37 °C. The number of colonies was normalized to the dilution factor and the mass of plasmid transformed to yield transformants per μ g of DNA. The relative transformation efficiency for each protospacer was calculated as a percentage of the transformation efficiency obtained for the empty vector control.

In assays shown in Fig. 2d, the parental strain in all cases is PA14 lacking the CRISPR2 locus due to CRISPR2-mediated inhibition which would prevent lysogeny of phages JBD30 and DMS3*m* lacking a functional anti-CRISPR. This was necessary so that phage JBD30 lacking its anti-CRISPR gene and phage DMS3*m* would be able to form lysogens. As shown in the left most column, the transformation efficiency of the construct bearing CR1_sp1 with PA14 CRISPR2 is approximately 10-fold less than the same construct in transforming WT PA14 (Fig. 1c). This is a consistent result, presumably due to the increased expression of crRNA from the CRISPR1 locus in the absence of CRISPR2 although this has not been explored.

DMS3 Recombination

Wild-type phage DMS3 contains a protospacer region in gene *42* with five mismatches to the 32 nt CR2_sp1 crRNA produced by PA14²⁰. A constructed mutant DMS3 phage (DMS3*m*) described previously¹⁴ as DMS3_{100%}, contains five point mutations in gene *42*

creating a 100% match to this crRNA. Due to targeting by the CRISPR/Cas system, this mutant phage is unable to form plaques on wild-type PA14, with the exception of rare ($<10^{-6}$) escaper mutants. Despite overall genomic similarity between phages DMS3*m* and JBD30, phage DMS3*m* does not contain an anti-CRISPR gene of its own. Therefore, DMS3*m* was used to generate a recombinant phage containing the anti-CRISPR gene from JBD30 (gene 35). Cells containing a pHERD20T construct containing JBD30 genes 34 to 38 (i.e. the anti-CRISPR gene from JBD30 with large flanking regions) were infected with DMS3*m* and recombinant phages were selected by plating on wild-type PA14. Individual plaques were picked and purified three times by re-plating on PA14, which ultimately led to the isolation of three independent recombinants. Preliminary screening involved PCR reactions with primers to the anti-CRISPR gene as well as primers to the protospacer region (gene 42) which were specific for a protospacer with 100% identity to the CR2_sp1 crRNA. Putative recombinant phages were then subject to three PCR reactions and subsequent sequencing. The protospacer containing region (gene 42) was sequenced to confirm that the recombinants had maintained 100% complementarity with the CR2_sp1 crRNA. The expected site of anti-CRISPR gene recombination (between DMS3 genes 29 and 31) was amplified using primers matching phage DMS3, outside of the region that was on the plasmid used for recombination and this was analyzed to identify the site of recombination (shown in Supplementary Fig. 12). The anti-CRISPR gene was also sequenced in recombinant phages to confirm that it was present and in-frame in all three recombinants (not shown). These reactions confirmed that the anti-CRISPR gene had been acquired and these phages were used in the experiments described here (Fig. 2c,d, Supplementary Fig. 12). Escapers were also identified with mutations in the protospacer and no recombination identified.

Northern Blot

Northern blots were conducted as described previously²⁰, with exceptions described below. WT PA14, PA14 *csy4*, PA14 *cr1/cr2* (both CRISPR loci deleted, *cas* genes intact) and PA14 lysogens were grown in LB. Total RNA was extracted from log phase cultures ($OD_{600nm}=0.8$) using the *mirVana* microRNA isolation kit (Ambion) and 5 μ g total RNA were run on a 10% TBE-Urea polyacrylamide gel and stained with SYBR Gold Nucleic Acid Gel Stain (Invitrogen) before transferring RNA to a nylon membrane at 200 mA for 1h. A radiolabelled probe corresponding to the last four spacers and three repeats of the PA14 CRISPR locus was generated²⁰. Prehybridization (blocking) was conducted using 50% formamide, 5 \times Denhardtts, 0.5% SDS, 6 \times SSC and 100 μ g/ml ssDNA at 42 $^{\circ}$ C for 2h. Probing was conducted at 42 $^{\circ}$ C for 16h using fresh prehybridization buffer, but with the ssDNA omitted and radiolabelled probe added. Wash solution 1 consisted of 2 \times SSC and 1% SDS while wash solution 2 consisted of 0.2 \times SSC and 0.1% SDS. Wash solution 1 was used for two 10 min washes at 25 $^{\circ}$ C, two 30 min washes at 65 $^{\circ}$ C, and wash solution 2 for one 10min wash at 25 $^{\circ}$ C. Blots were developed using a phosphor screen and imager. A low range ssRNA ladder (NEB) was also used to confirm the location of 5S RNA and crRNA.

Reverse Transcriptase Quantitative PCR (RT-qPCR)

Total RNA extracts were treated with DNase (Ambion) to remove DNA and 1ng of total RNA was used in a series of RT-qPCR reactions. Reactions were conducted in an Eppendorf

qPCR cycler, using VWR white plates with the SensiFAST No-ROX One-step Kit (Bioline). For the purposes of absolute quantification, a PCR reaction was conducted, amplifying genomic DNA with 'external' primers. This product was gel extracted, quantified and diluted to generate a standard curve. All RT-qPCR reactions were done with 'internal' primers which were designed to anneal inside of the external primers for the purified PCR product. A housekeeping gene, *rpsL*, was used for relative quantification. For RT-qPCR reactions, 1 ng of total RNA was used in each reaction, performed in duplicate. Reverse transcription was conducted using a gene specific primer to generate cDNA in a one-step reaction. The lack of contaminating DNA was confirmed by inclusion of controls for each sample without reverse transcriptase added.

β -Galactosidase Assays

Overnight cultures were subcultured 1:100 into LB containing 0.1% arabinose to induce anti-CRISPR gene expression from the pHERD30T plasmid, and then grown at 37°C to an OD_{600nm} of 0.3–0.6. Cultures were diluted 1:1 in complete Z buffer, in triplicate. Two drops each of 0.1% SDS and chloroform were added to each sample and after vortexing, 200 μ l ONPG was added. Samples were vortexed to begin the reaction, and then incubated at 30°C without shaking for 20–30 minutes. Absorbance measurements were taken at 420 and 550 nm, and β -galactosidase activity was calculated for each technical replicate using the Miller equation. Data are expressed relative to cells containing the pHERD30T empty vector for at least five biological replicates.

Anti-CRISPR Knockout

Three independent PCR products were generated which contained overhangs (O/H), that facilitated the generation of a pHERD20T (Amp^R, 20T) plasmid with the region from phage JBD30 that lies up and downstream of the anti-CRISPR (gene *35*) along with an inserted gentamicin (Gm) resistance cassette and the first 60bp of gene *35* absent. Primers used are outlined in Supplementary Table 3.

Product 1: Gene *34* with 5' O/H to 20T, 3' O/H to Gm.

Product 2: Gm cassette with 5' O/H to Gene *34*, 3' O/H to Gene *35* (lacking first 60bp). Product 3: Gene *35* (lacking first 60bp) with 5' O/H to Gm, 3' O/H to 20T.

All three PCR products were gel purified and amplified together in a reaction with Vent DNA Polymerase using primers pHERD-34-F and pHERD-36-R. This reaction yielded a DNA product that was gel extracted and reamplified with Taq DNA polymerase. The pHERD20T vector was digested with *EcoRI* and *HindIII* and the infused using the IN-Fusion EcoDry cloning kit (Clontech) following the manufacturers instructions. The mixture was used to transform *E. coli* DH5 α using standard protocols with recovery in SOC followed by plating and selection with ampicillin. Plasmids were isolated from colonies that were both gentamicin- and ampicillin-resistant and confirmed by sequencing and diagnostic restriction enzyme digestion. The plasmid containing a gentamicin resistance cassette, flanked by regions of homology to the 300 bp upstream and downstream of the coding region of JBD30 gene *35* was electroporated into a PA14 CR/*cas*(JBD30) lysogen to generate recombinant phages. Isolated gentamicin resistant colonies were grown in liquid

culture to allow phage production and a cell free phage preparation from the supernatant was used to infect CR/*cas* cells overnight in liquid culture. Surviving cells were plated on gentamicin to select for newly formed CR(JBD30) lysogens with a prophage containing the gentamicin insert in gene *35*. Resulting colonies were confirmed to be gentamicin resistant and carbenicillin sensitive (confirming no plasmid transfer had occurred). The correct insertion of the gentamicin cassette in the phage genome was confirmed by PCR and DNA sequencing. The presence of the gentamicin cassette in the phage created plaques that were smaller, more turbid and required prolonged incubation. To remove the cassette, pHERD20T containing JBD30 genes *34–38* with either wild-type sequence or a frameshift introduced in gene *35* were electroporated into the knockout strain under carbenicillin selection. Single colonies were grown in liquid and plaque assays conducted with the supernatant to identify for recombinants. Plaques with wild-type morphology and growth kinetics were picked, purified, and confirmed by PCR and sequencing to contain either the wild-type sequence or a frameshift mutation in gene *35* corresponding to the input vector.

The frameshift mutation in JBD30 gene *35* was introduced into pHERD20T containing JBD30 genes *34–38* with a PCR reaction with primers 30–35fsF/R. Eighteen cycles were conducted with 9 minute extension time using Pfu DNA polymerase and subsequent *DpnI* digest to remove parental plasmid.

Type I-E CRISPR/Cas System Assays

1.5 ml of an overnight culture washed twice with 1ml of ice cold sterile water, washed once with 1 ml of ice cold 10% glycerol, and resuspended in 100 μ l ice cold 10% glycerol. ~300 ng of plasmid was electroporated and the cells recovered. Cells were then centrifuged, resuspended in 100 μ l LB medium, and plated on LB agar plates containing 15 μ g/ml gentamicin. Plates were grown overnight at 37 °C. Overnight cultures of *E. coli* BW40114 and BW40119¹⁹ containing the empty vector or anti-CRISPR genes were diluted 100-fold into LB medium containing 15 μ g/ml gentamicin and grown at 37 °C for four hours. Isopropyl- β -D-thiogalactoside (IPTG) and arabinose were then added to a final concentration of 1 mM each. The cultures were grown under induction for two hours, then 1.5 ml of each culture was concentrated into 100 μ l and mixed with 3 ml molten LB soft agar. The mixture was poured onto thick LB agar plates containing 15 μ g/ml gentamicin, 1 mM IPTG, and 1 mM arabinose. Ten-fold serial dilutions of M13 phage lysate were spotted onto the plates and incubated overnight at 30 °C. Lysates which were produced from targeting cells (BW40119) containing anti-CRISPR constructs or empty vector (ev) under conditions in which the plasmid promoter was repressed (–, 0.2% glucose) or induced (+, 1mM arabinose) and analyzed by SDS-PAGE to assess the expression of anti-CRISPR proteins.

Supplementary Material

Refer to Web version on PubMed Central for supplementary material.

Acknowledgments

The authors would like to thank David Guttman, You-Hee Cho, Kyle Cady, and George O'Toole for providing *P. aeruginosa* strains and phages. We also thank Konstantin Severinov for providing the M13 phage and *E. coli* strains required for assaying the Type 1-E system. We thank John Brumell, Andrew Spence, and William Navarre for critical reading of the manuscript. We also thank Diane Bona for technical assistance. This work was supported by an Operating Grant to K.L.M. (Fund No. MOP- 6279) and an Emerging Team Grant to A.R.D. and K.L.M. (Fund No. XNE86943) both of which are from the Canadian Institutes for Health Research. J.B.D. was supported by a CIHR Canada Graduate Scholarship Doctoral Award.

References

1. Makarova KS, et al. Evolution and classification of the CRISPR-Cas systems. *Nat Rev Micro*. 2011; 9:467–477.
2. Makarova KS, Grishin NV, Shabalina SA, Wolf YI, Koonin EV. A putative RNA-interference-based immune system in prokaryotes: computational analysis of the predicted enzymatic machinery, functional analogies with eukaryotic RNAi, and hypothetical mechanisms of action. *Biol Direct*. 2006; 1:7. [PubMed: 16545108]
3. Brouns SJJ, et al. Small CRISPR RNAs Guide Antiviral Defense in Prokaryotes. *Science*. 2008; 321:960–964. [PubMed: 18703739]
4. Rodriguez-Valera F, et al. Explaining microbial population genomics through phage predation. *Nat Rev Micro*. 2009; 7:828–836.
5. Labrie SJ, Samson JE, Moineau S. Bacteriophage resistance mechanisms. *Nat Rev Micro*. 2010; 8:317–327.
6. Jore MM, Brouns SJJ, van der Oost J. RNA in Defense: CRISPRs Protect Prokaryotes against Mobile Genetic Elements. *Cold Spring Harb Perspect Biol*. 4:2012.
7. Haurwitz RE, Jinek M, Wiedenheft B, Zhou K, Doudna JA. Sequence- and Structure-Specific RNA Processing by a CRISPR Endonuclease. *Science*. 2010; 329:1355–1358. [PubMed: 20829488]
8. Deltcheva E, et al. CRISPR RNA maturation by trans-encoded small RNA and host factor RNase III. *Nature*. 2011; 471:602–607. [PubMed: 21455174]
9. Wiedenheft B, et al. Structures of the RNA-guided surveillance complex from a bacterial immune system. *Nature*. 2011; 477:486–489. [PubMed: 21938068]
10. Westra ER, et al. CRISPR Immunity Relies on the Consecutive Binding and Degradation of Negatively Supercoiled Invader DNA by Cascade and Cas3. *Mol Cell*. 2012; 46:595–605. [PubMed: 22521689]
11. Garneau JE, et al. The CRISPR/Cas bacterial immune system cleaves bacteriophage and plasmid DNA. *Nature*. 2010; 468:67–71. [PubMed: 21048762]
12. Barrangou R, et al. CRISPR provides acquired resistance against viruses in prokaryotes. *Science*. 2007; 315:1709–1712. [PubMed: 17379808]
13. Yosef I, Goren MG, Qimron U. Proteins and DNA elements essential for the CRISPR adaptation process in *Escherichia coli*. *Nucleic Acids Res*. 2012; 40:5569–5576. [PubMed: 22402487]
14. Cady KC, Bondy-Denomy J, Heussler GE, Davidson AR, O'Toole GA. The CRISPR/Cas Adaptive Immune System of *Pseudomonas aeruginosa* Mediates Resistance to Naturally Occurring and Engineered Phages. *J Bacteriol*. 2012; 194:5728–5738. [PubMed: 22885297]
15. Marraffini LA, Sontheimer EJ. Self versus non-self discrimination during CRISPR RNA-directed immunity. *Nature*. 2010; 463:568–571. [PubMed: 20072129]
16. Mojica FJM, Diez-Villasenor C, Garcia-Martinez J, Almendros C. Short motif sequences determine the targets of the prokaryotic CRISPR defence system. *Microbiology*. 2009; 155:733–740. [PubMed: 19246744]
17. Braid MD, Silhavy JL, Kitts CL, Cano RJ, Howe MM. Complete genomic sequence of bacteriophage B3, a Mu-like phage of *Pseudomonas aeruginosa*. *J Bacteriol*. 2004; 186:6560–6574. [PubMed: 15375138]
18. Morgan GJ, Hatfull GF, Casjens S, Hendrix RW. Bacteriophage Mu genome sequence: analysis and comparison with Mu-like prophages in *Haemophilus*, *Neisseria* and *Deinococcus*. *J Mol Biol*. 2002; 317:337–359. [PubMed: 11922669]

19. Datsenko KA, et al. Molecular memory of prior infections activates the CRISPR/Cas adaptive bacterial immunity system. *Nat Commun.* 2012; 3:945. [PubMed: 22781758]
20. Cady KC, O'Toole GA. Non-Identity-Mediated CRISPR-Bacteriophage Interaction Mediated via the Csy and Cas3 Proteins. *J Bacteriol.* 2011; 193:3433–3445. [PubMed: 21398535]
21. Battle SE, Meyer F, Rello J, Kung VL, Hauser AR. Hybrid pathogenicity island PAGI-5 contributes to the highly virulent phenotype of a *Pseudomonas aeruginosa* isolate in mammals. *J Bacteriol.* 2008; 190:7130–7140. [PubMed: 18757543]
22. Cady KC, et al. Prevalence, conservation and functional analysis of *Yersinia* and *Escherichia* CRISPR regions in clinical *Pseudomonas aeruginosa* isolates. *Microbiology.* 2011; 157:430–437.
23. Semenova E, et al. Interference by clustered regularly interspaced short palindromic repeat (CRISPR) RNA is governed by a seed sequence. *Proc Natl Acad Sci USA.* 2011; 108:10098–10103. [PubMed: 21646539]
24. Wiedenheft B, et al. RNA-guided complex from a bacterial immune system enhances target recognition through seed sequence interactions. *Proc Natl Acad Sci USA.* 2011; 108:10092–10097. [PubMed: 21536913]
25. Zegans ME, et al. Interaction between bacteriophage DMS3 and host CRISPR region inhibits group behaviors of *Pseudomonas aeruginosa*. *J Bacteriol.* 2009; 191:210–219. [PubMed: 18952788]
26. Heo YJ, Chung IY, Choi KB, Lau GW, Cho YH. Genome sequence comparison and superinfection between two related *Pseudomonas aeruginosa* phages, D3112 and MP22. *Microbiology.* 2007; 153:2885–2895. [PubMed: 17768233]
27. Chung IY, Cho YH. Complete Genome Sequences of Two *Pseudomonas aeruginosa* Temperate Phages, MP29 and MP42, Which Lack the Phage-Host CRISPR Interaction. *J Virol.* 2012; 86:8336. [PubMed: 22787268]
28. Wang PW, Chu L, Guttman DS. Complete sequence and evolutionary genomic analysis of the *Pseudomonas aeruginosa* transposable bacteriophage D3112. *J Bacteriol.* 2004; 186:400–410. [PubMed: 14702309]
29. Aziz RK, et al. The RAST Server: rapid annotations using subsystems technology. *BMC Genomics.* 2008; 9:75. [PubMed: 18261238]
30. Larkin MA, et al. Clustal W and Clustal X version 2.0. *Bioinformatics.* 2007; 23:2947–2948. [PubMed: 17846036]
31. Qiu D, Damron FH, Mima T, Schweizer HP, Yu HD. PBAD-Based Shuttle Vectors for Functional Analysis of Toxic and Highly Regulated Genes in *Pseudomonas* and *Burkholderia* spp and Other Bacteria. *Applied and Environmental Microbiology.* 2008; 74:7422–7426. [PubMed: 18849445]

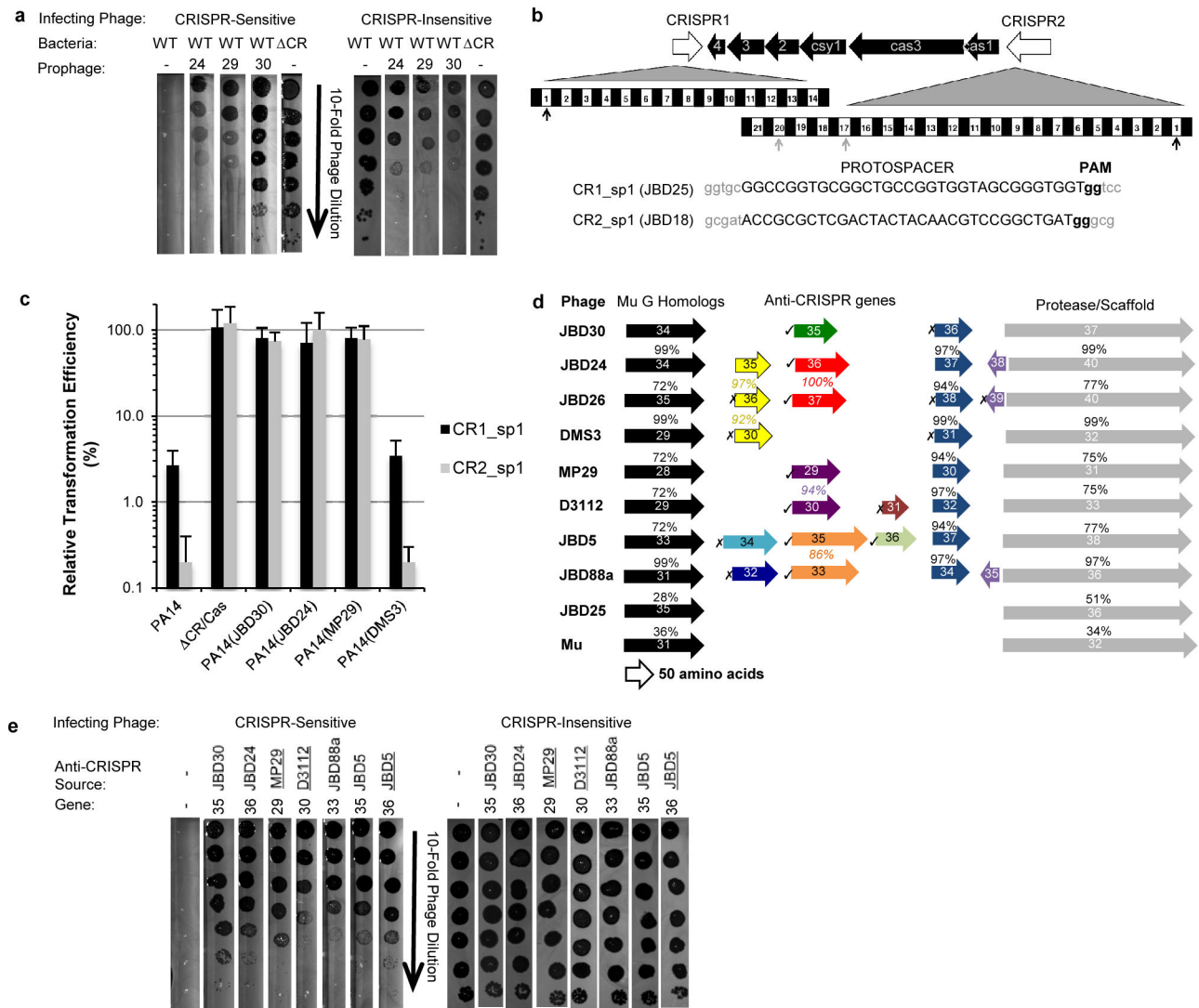


Figure 1. The CRISPR/Cas system is inhibited by expression of phage genes

a, Ten-fold dilutions of lysates of a CRISPR-sensitive phage (JBD18) and a CRISPR-insensitive phage (DMS3) were applied to bacterial lawns of wild-type (WT) PA14, PA14 lysogens (JBD24, MP29, or JBD30), and PA14 lacking a CRISPR/Cas system (Δ CR/cas). **b**, A schematic of the PA14 CRISPR loci and *cas* gene region is shown. Expanded versions of each CRISPR locus indicate the number of spacers in each, shown with white boxes, each of which is flanked by repeats denoted by black boxes. Black arrows indicate the CRISPR spacers corresponding to protospacers tested in Fig. 1c and gray arrows indicate the CRISPR spacers corresponding to protospacers tested in Supplementary Fig. 11. The DNA sequences of the protospacers tested in Fig. 1c are shown. **c**, Plasmids containing protospacers shown in Fig. 1b were electroporated into the indicated strains. The relative transformation efficiency was calculated by comparison with the transformation efficiency of the cloning vector containing no protospacer insert. Error bars represent standard deviation from the mean of three biological replicates. **d**, The anti-CRISPR genes of the indicated phages are located in the head gene regions of these genomes between genes homologous to the *G* gene

of *E. coli* phage Mu (black boxes) and genes encoding the protease/scaffold protein of the phage head (gray boxes; see Supplementary Fig. 2). The percent identity of the proteins encoded by these genes to representatives from JBD30 are shown. The coloured boxes represent putative anti-CRISPR genes. Boxes of the same colour represent closely related genes and the sequence identity of their encoded proteins is indicated. Genes found to mediate anti-CRISPR activity are indicated by check marks and genes tested but displaying no anti-CRISPR activity are marked with an “X”. Unmarked genes were not tested due to their high similarity to tested genes. The gene box sizes are proportional to the sizes of the proteins in question (scale bar is 50 amino acids), but the spacing of the genes is not to scale. **e**, The same phages from Fig. 1a were tested on PA14 containing empty vector or plasmids expressing the indicated anti-CRISPR genes. Induction of the plasmid promoter with arabinose was required to produce a maximal effect for some of the anti-CRISPR genes as indicated by underlining. The assays shown in Fig. 1a,e are by necessity taken from different plates. The complete plates for these experiments and experiments with the other CRISPR-sensitive phages are shown in Supplementary Fig. 1.

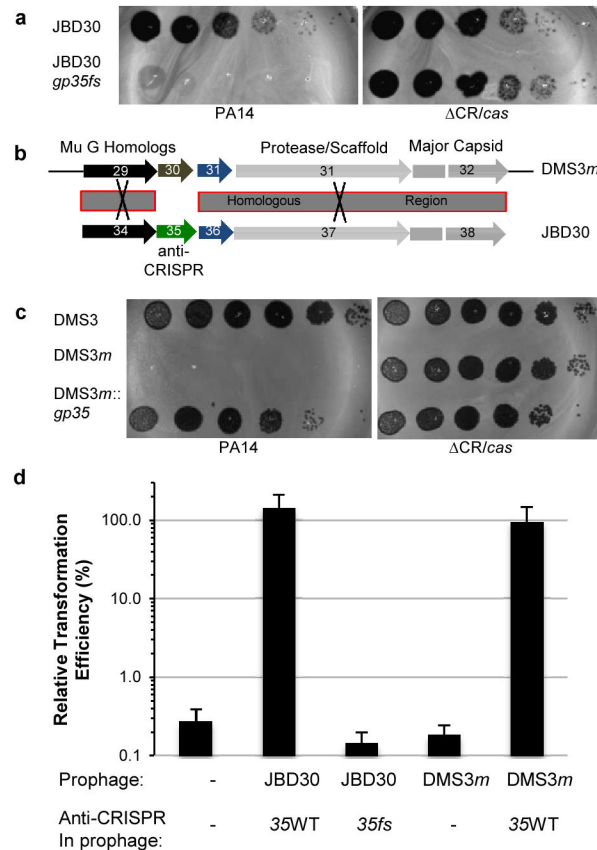


Figure 2. An anti-CRISPR gene protects phages from the CRISPR/Cas system during infection
a, Ten-fold dilutions of lysates of anti-CRISPR phage JBD30, and the same phage with a frameshift mutation introduced into the anti-CRISPR gene *35* (gene *35fs*) were applied to lawns of PA14 or PA14 Δ CR/*cas*. This experiment was carried out in a manner similar to those shown in Fig. 1a. **b**, A schematic representation of the *in vivo* homologous recombination between phage DMS3*m* and the anti-CRISPR region from phage JBD30. The X marks approximate the mapped region of recombination, up- and downstream of the anti-CRISPR gene *35* from JBD30 with details shown in Supplementary Fig. 12 and Methods. **c**, Ten-fold dilutions of lysates of a CRISPR-insensitive phage (DMS3), a CRISPR-sensitive phage (DMS3*m*), and DMS3*m* with anti-CRISPR gene *35* from JBD30 inserted (DMS3*m*::gene *35*) were applied to lawns of PA14 or PA14 Δ CR/*cas*. **d**, A plasmid containing a protospacer matching CR1_sp1 (shown in Fig. 1b) was electroporated into the indicated lysogens or parent strain. As indicated, the prophages within these lysogens contain either a wild-type (WT) version of anti-CRISPR gene *35*, a frameshift mutant of this gene, or no anti-CRISPR gene.